LAWRENCE
LIVERMORE
NATIONAL
LABORATORY

LLNL-JRNL-565076

Redefining the microbial niche based on taxon-specific response to differing substrate concentration

X. Mayali, P. K. Weber, J. Pett-Ridge, S. Mabery

July 18, 2012

PLoS ONE

Disclaimer

BIOLOGICAL SCIENCES: Environmental Science and Ecology

Redefining the microbial trophic niche based on response to differing substrate concentrations

Xavier Mayali[a,†], Peter K. Weber[a], Shalini Mabery, Jennifer Pett-Ridge[a,]

[a]Physical and Life Science Directorate, Lawrence Livermore National Laboratory, 7000 East Ave, Livermore CA 94550

[†]To whom correspondence should be addressed. E-mail: mayali1@llnl.gov

Abstract

The trophic strategies of aquatic microorganisms are characterized as oligotrophic and copiotrophic, adapted to low and high nutrient concentrations, respectively. We tested whether this hypothesis applied to co-occurring microbial populations using incubations with stable isotope labeled amino acids at concentrations spanning three orders of magnitude, followed by taxon-specific quantitative analysis of isotopic incorporation with Chip-SIP. We uncovered at least seven distinct trophic strategies, mathematically defined according to the combination of activity level and substrate concentration optimum. These data allowed the further separation of microbial guilds based on high or low activity, wide or narrow concentration optima, and intermediate or extreme concentration optima. This unexpected range of adaptive strategies to resource availability highlights our need to expand our understanding of microbial interactions with organic matter in order to better predict microbial responses to a changing environment. Our results suggest that concentration-dependent substrate utilization is a factor in microbial niche differentiation with implications for our understanding of microbial ecology, evolution, and biogeochemical cycling.

Microbes dominate the biomass and biogeochemical activity of aquatic environments on a global scale (1), but our mechanistic understanding of their physiological coupling with their resources is incomplete. Most aquatic microbes are osmotrophic bacteria harboring cell-bound but extracellular enzymes that interact directly with dissolved substrates on a molecular level (2). Individual microbial cells can harbor multiple transporters for the same substrate, and these different transporters have substrate-binding efficiencies adapted to different concentrations (3). This allows microorganisms to respond to the resource patchiness of seawater (4) through, among other things, niche differentiation. For example, in the case of ammonia oxidation in certain environments, one major group of organisms (ammonia-oxidizing bacteria) is thought to dominate activity at higher ammonium concentrations and another (ammonia-oxidizing archaea) dominate activity at lower concentrations (5). Other evidence exists that ammonium and phosphate uptake at higher concentations (> nanomolar) is dominated by larger organisms, whereas at lower (nanomolar) concentrations, smaller organisms (< 1 micron) dominate the uptake (6). In greater phylogenetic detail, previous work has also suggested that phylum-level microbial taxa respond differently to different concentrations of leucine (7), in particular during different stages of an algal bloom.

In the context of both inorganic nutrient and organic substrate acquisition, microbes (bacteria in particular) have been classified into two main guilds with respect to their adaptation to substrate concentrations: oligotrophs and copiotrophs (8), the latter also referred to as opportunitrophs (9). Oligotrophs are generally small cells with small genomes and are characterized by slow, steady growth, while copiotrophs, with larger cells and more extensive genomes, subsist on a feast-or-famine approach (fast growth

54 interspersed with inactivity) (10). While the use of these terms has been quite beneficial
55 for our conceptual understanding of microbial biogeochemical cycling, there are likely
56 additional microbial trophic strategies yet to be uncovered.

57 We set out to examine whether the simple classification scheme of oligotroph vs.
58 copiotroph could be expanded to more fully categorize the range of microbial substrate
59 utilization strategies enabling microbes to co-exist through trophic niche differentiation.
60 Our goal was to test how microbial taxa responded in their incorporation of amino acids
61 (AAs), organic substrates commonly utilized by aquatic microorganisms (11, 12), added
62 at three different concentrations. To achieve this goal, we used Chip-SIP, a method
63 capable of quantifying taxon-specific relative incorporation of stable isotope labeled
64 substrates (13). We incubated San Francisco Bay estuarine samples in glass bottles with
65 ^{15}N labeled mixed AAs for 12 hrs at concentrations of 5 μM, 500 nM, and 50 nM, in the
66 range of AA concentrations measured in estuaries (14). Using NanoSIMS image analysis
67 of the extracted RNA hybridized to microarrays targeting over one hundred rRNA
68 phylotypes, we measured the relative isotopic enrichment of these taxa at each substrate
69 concentration. These data provided two types of information: 1) relative activity among
70 taxa, for any substrate concentration, and 2) for each taxon, relative activity among the
71 three concentrations tested. Though we had no *a priori* expectations, we envisioned
72 several possible outcomes. The null hypothesis is that all taxa would incorporate the
73 labeled AAs comparably regardless of concentration. One alternative hypothesis is that
74 all taxa would incorporate more substrate with increasing concentration. Another
75 alternative is that we would be able to identify microbial groups with higher relative

76 incorporation at the higher concentrations (copiotrophs), and others with higher relative
77 incorporation at the lower concentrations (oligotrophs).

78

79 **Results and Discussion**

80 Comparison of two concentrations

81 Our results revealed an unexpectedly high degree of complexity in the microbial
82 community response to varying AA concentrations. We initially restricted our
83 examination of the data from two concentrations (5μM and 50 nM, corresponding to high
84 and low, respectively; Fig. 1a). Generally, incorporation at high AA concentration was
85 correlated to incorporation at low concentration, meaning that phylotypes with high
86 activity at the high substrate concentration also had high activity at the low concentration
87 (and vice-versa; linear regression analysis was significant with $R^2 = 0.56$). Significant
88 deviations from this relationship towards the high concentration or towards the low
89 concentration imply a copiotrophic or oligotrophic strategy, respectively (Fig. 1a). In
90 other words, phylotypes with statistically higher relative incorporation at the high
91 substrate concentration were considered copiotrophs, and those with higher relative
92 incorporation at the lower substrate concentration were considered oligotrophs. Other
93 phylotypes exhibited equal incorporation at the high and low concentrations; we named
94 these eurytrophs ("eury" for "wide" concentration optimum). We also identified a
95 contrast between a few phylotypes with high activity (away from the origin along the
96 regression line on Fig. 1a), which we named hypertrophs ("hyper" for "over"), from the
97 rest of the phylotypes with relatively low activity, which we named hypotrophs ("hypo"
98 for "below"). We considered phylotypes to be hypertrophs if their activity was more than

99 50% of the highest activity recorded (Fig. S1, S2). In this set of experiments, all
100 hypertrophs were members of the *Roseobacter* group, a subclade of the Alpha
101 Proteobacteria that play key biogeochemical roles in the ocean (15) and are believed to be
102 substrate generalists (16). We note here that relative response to substrate concentration
103 (oligotrophy vs. copiotrophy vs. eurytrophy) and relative activity level (hypotrophy vs.
104 hypertrophy) are independent of one another. In other words, eurytrophs can be either
105 hypo-eurytrophs or hyper-eurytrophs, and so on. Comparisons between the medium
106 concentration tested (500 nM) and the high and low concentrations generally showed
107 similar results (Fig. 1b, 1c). One conspicuous feature, however, became apparent when
108 comparing activity between two concentrations with phylotypes color-coded by higher
109 taxonomic level. In particular, Gamma Proteobacteria and Bacteroidetes appeared to
110 exhibit a dissimilar distribution. For example, when comparing the low concentration to
111 the high and to the medium (Figs 1a and 1c), Gamma Proteobacteria appeared to be more
112 copiotrophic than Bacteroidetes. However, when comparing the medium concentration to
113 the high (Fig. 1b), it was the reverse: Bacteroidetes appeared to be more copiotrophic
114 than Gamma Proteobacteria. In order to resolve this inconsistency, it became necessary to
115 examine the AA incorporation response to the three concentrations simultaneously.

116

117 Comparison of three concentrations

118 An additional level of complexity arose when comparing three concentrations vs.
119 comparing just two. For example, some phylotypes exhibited higher incorporation at the
120 high concentration compared to the medium and low (i.e. H>M=L), and others higher
121 incorporation at the high and medium concentrations compared to the low (H=M>L). We

122 considered both of these cases different versions of copiotrophy (the first having a wide
123 concentration optimum, the second with a narrow one). The cases of oligotrophy were
124 treated similarly. We plotted phylotype-specific relative incorporation for the three AA
125 concentrations on ternary diagrams (Fig. 2), which graphically depict the ratios of three
126 variables on an equilateral triangle. In this case, the variables are the relative responses to
127 high, medium, and low AA concentrations, and for each phylotype, the three variables
128 add up to a constant. We note that activity level (i.e. hyper vs hypotrophy) is not taken
129 into account here, but only the response to substrate concentrations (oligo vs. copio vs.
130 eurytrophy). If a phylotype is a copiotroph, it will be graphed away from the center of the
131 plot, towards the high concentration (bottom left corner of the triangle); this is
132 represented by the red background color in Fig. 2. Oligotrophs will be plotted towards the
133 low concentration (green background color), and eurytrophs will be placed in the center
134 of the plot. Based on the remaining areas of the plot that do not mathematically represent
135 copiotrophic or oligotrophic lifestyles, we identified two other potential trophic
136 strategies. The first is where relative incorporation is higher at the medium concentration
137 than the high and low, which we call mesotrophic ("meso" for "middle"), represented by
138 the yellow background area in Fig. 2. The second is where relative incorporation is higher
139 at the high and low concentrations compared to the medium, which we call allotrophic
140 ("allo" for "different"), represented by the orange background color. To determine
141 whether phylotypes could be assigned to these two new trophic strategies, we used a
142 simple model incorporating statistical analyses of the quantitative isotopic incorporation
143 data to assign each taxon to a guild (Fig. S1, S2). For example, in order to be assigned as
144 a mesotroph, a phylotype had to exhibit significantly greater isotopic incorporation at the

145 medium concentration compared to the high and the low. Phylotypes assigned to a
146 trophic status by the model are displayed individually on ternary diagrams in Figs. 2b-e.
147 Several were statistically assigned as mesotrophs and allotrophs, having concentration
148 optima in the middle or at the extremes, respectively. This phenomenon is analogous to
149 the concept of stabilizing versus disruptive selection in evolutionary biology occurring on
150 longer timescales, where over many generations, a trait becomes either more prevalent at
151 the intermediate phenotype (stabilizing) or at the two extreme phenotypes (disruptive)
152 (17).

153

154 Phylogenetic distribution of trophic strategy

155 To examine whether phylogeny was correlated to trophic lifestyle, we mapped the
156 trophic strategies identified by the model onto a phylogenetic tree of the 16S rRNA gene
157 (Fig. 3). Several patterns were noticeable. Bacteroidetes were either copiotrophs or
158 allotrophs (with one eurytroph exception), while Gamma Proteobacteria were all
159 eurytrophs or copiotrophs. Alpha Proteobacteria, including *Roseobacters,* exhibited all
160 strategies except mesotrophy. We determined whether strategies were statistically
161 restricted to certain parts of the tree using a reshuffling analysis. This involves mapping
162 one character state at a time (e.g. copiotroph vs. not copiotroph, etc), calculating the
163 number of character state changes on the phylogenetic tree (i.e. a parsimony score), and
164 then reshuffling the characters 1000 times and calculating the character state changes for
165 each reshuffling. If the character state change for the real state is significantly different
166 than the reshuffled distribution, then that character is clustered as opposed to randomly
167 distributed. Only one strategy (copiotrophy) showed a statistically significant difference

168 from the random distribution (Fig. S3), meaning that it was clustered. This implies that
169 copiotrophy is under selection, which is perhaps not surprising given the source of this
170 community, a nutrient-rich estuary, where selection for high substrate uptake might be
171 beneficial. Our analysis did not detect significant clustering of the other trophic
172 strategies, suggesting they may not be under strong selective pressure in this ecosystem.

173

174 Conclusion

175 Our results suggest that in addition to spatial and resource partitioning (18), microbial
176 niche differentiation based on different substrate affinities is a factor that contributes to
177 the maintenance of diversity in aquatic environments. In a eutrophic ecosystem, with
178 three concentrations of one organic substrate, we uncovered more complex trophic
179 strategies than the previously identified dichotomy of oligotrophy vs. copiotrophy. The
180 seven strategies statistically identified here (hypercopiotrophy, hypereurytrophy,
181 hypoallotrophy, hypocopiotrophy, hypoeurytrophy, hypomesotrophy, and
182 hypooligotrophy; Fig. S4) most likely still represent an oversimplification of the trophic
183 lifestyles of bacteria. For example, we can easily imagine many more strategies if we had
184 tested more concentrations, two or more substrates, and different environments. Given
185 the complexity of dissolved organic matter (19), representing potentially hundreds of
186 thousands of different kinds of molecules available to microbial cells, our results appear
187 daunting if the goal is to understand the interaction between microbes and their resources.
188 On the other hand, our analysis demonstrates that the complex substrate incorporation
189 patterns of natural mixed microbial communities can be quantified and used in
190 moderately simple classification schemes, leading to an improvement in how microbial

191 populations are assigned to functional guilds. The categorization of microbes into an
192 increasing number of "boxes" (here increasing from two to seven) is valuable for several
193 reasons, two of which we briefly discuss here. First, biogeochemical models, when they
194 consider bacteria, usually have one box to represent the vast diversity of heterotrophic
195 processes (20). Expanding the bacterial "black box" should increase the accuracy and
196 usefulness of such models. Second, one of the goals of microbial ecology is to understand
197 the distribution, abundance, and ecological roles of microbes, but this is difficult to do
198 when we do not understand which microbes behave similarly. Categorizing organisms
199 with similar functional traits into boxes allows us to strengthen our conceptual
200 understanding of the processes they mediate, such as carbon cycling. However, the
201 number of boxes needs to be relatively low or we lose our ability for this conceptual
202 understanding. For example, we can easily conceptualize microbes based on their
203 temperature tolerance, such as thermophiles, mesophiles, and psychrophiles (21), being
204 adapted to high, medium, and low temperature, respectively. However, it is difficult to
205 conceptualize ten or twenty such groups (e.g. those that prefer 70-80°C, 60-70°C, 50-
206 60°C, and so on). The reason for this is likely related to the maximum number of items
207 the conscious human mind can simultaneously store, which is only four (22). While our
208 analysis resulted in seven guilds, we note that they were created based on the
209 combination of two separate concepts (activity level and concentration optimum), with
210 each concept having two (hyper, hypo) and five (oligo, copio, allo, meso, eury) states,
211 respectively. This approach of combining concepts to assign microbes to more than four
212 functional groups allows us to retain a conceptual understanding of their functional
213 categories.

214 **Materials and Methods:**

215 **Incubation of field samples.** Surface water was collected at the public pier in
216 Berkeley, CA USA (37°51'46.67″N, 122°19'3.23″W) and brought back to the laboratory
217 within one hour in a cooler. Glass bottles (500 ml) were filled without air space and dark
218 incubated at 14°C. Samples were incubated in triplicate bottles with 5 μM, 500 nM, and
219 50 nM mixed amino acids (99 atm % ^{15}N labeled; Omicron), collected by filtration after
220 12 hrs and frozen at -80°C. RNA extracts from triplicate incubations were combined and
221 hybridized to the array (as described below) for subsequently NanoSIMS analysis. RNA
222 extracts from all three treatments (high, medium, and low) were combined for fluorescent
223 labeling (see below) in order to compare the three concentration treatments to one
224 another.

225 **RNA extraction and labeling.** RNA from frozen filters was extracted with the
226 Qiagen RNEasy kit according to manufacturer's instructions. RNA samples were split:
227 one fraction saved for fluorescent labeling, the other was unlabeled for NanoSIMS
228 analysis. Alexafluor 532 labeling was done with the Ulysis kit (Invitrogen) for 10 min at
229 90°C (2 μL RNA, 10 μL labeling buffer, 2 μL Alexafluor reagent), followed by
230 fragmentation. All RNA (fluorescently labeled or not) was fragmented using 1X
231 fragmentation buffer (Affymetrix) for 10 min at 90°C before hybridization and
232 concentrated by isopropanol precipitation to a final concentration of 500 ng μL^{-1}.

233 **Microarray hybridization and NanoSIMS.** We targeted the microbial
234 community from San Francisco Bay with approximately 25 probes for each taxon XM
235 REF. Glass slides coated with indium-tin oxide (ITO; Sigma) were coated with silane
236 Super Epoxy 2 (Arrayit Corporation) to provide a starting matrix for DNA synthesis.

237 Custom-designed microarrays (spot size = 17 μm) were synthesized using a photolabile
238 deprotection strategy (23) on the LLNL Maskless Array Synthesizer (Roche Nimblegen,
239 Madison, WI). Reagents for synthesis (Roche Nimblegen) were delivered through the
240 Expedite (PerSeptive Biosystems) system. These arrays are also available directly from
241 Roche Nimblegen by special order. For array hybridization, RNA samples (1 μg) in 1X
242 Hybridization buffer (Roche Nimblegen) were placed in Nimblegen X4 mixer slides and
243 incubated inside a Maui hybridization system (BioMicro® Systems) for 18 hrs at 42 °C
244 and subsequently washed according to manufacturer's instructions (Roche Nimblegen).
245 Arrays with fluorescently labeled RNA were imaged with a Genepix 4000B fluorescence
246 scanner at pmt = 650 units.

247 Secondary ion mass spectrometry analysis of microarrays hybridized with ^{15}N
248 rRNA was performed at LLNL with a Cameca NanoSIMS 50 (Cameca, Gennevilliers,
249 France). A Cs+ primary ion beam was used to enhance the generation of negative
250 secondary ions. Nitrogen isotopic ratios were determined by electrostatic peak switching
251 on electron multipliers in pulse counting mode, alternately measuring $^{12}C^{14}N^-$ and $^{12}C^{15}N^-$
252 simultaneously. More details of the instrument parameters are provided elsewhere (13).
253 Ion images were stitched together and processed to generate isotopic ratios with custom
254 software (LIMAGE, L. Nittler, Carnegie Institution of Washington). Isotopic ratios were
255 converted to delta (permil) values using $\delta = [(R_{meas}/R_{standard}) - 1] \times 1000$, where R_{meas} is
256 the measured ratio and $R_{standard}$ is the standard ratio (0.00367 for $^{15}N/^{14}N$). Data were
257 corrected for the natural abundance ratios measured in unhybridized locations of the
258 sample.

259 **Data analyses**. For each phylotype, isotopic enrichment of individual probe spots
260 was plotted versus probe fluorescence and a linear regression slope was calculated with
261 the y-intercept constrained to natural isotope abundances (zero permil). This calculated
262 slope (permil/fluorescence), which we refer to as the hybridization-corrected enrichment
263 (HCE, is a metric that can be used to compare the relative incorporation of a given
264 substrate by different taxa.

265 Two procedures were carried out to assign phylotypes to guilds according to AA
266 incorporation patterns. First, taxa were assigned to groups based on activity level, defined
267 by HCE values. We note that this assignment does not take into consideration the
268 response to different substrate concentrations. The HCE values at a single concentration
269 followed a lognormal distribution with a small number of high values and mostly low to
270 intermediate values (Fig. S1a). While the distribution of HCEs represents a continuum of
271 activity, for simplicity we aimed to separate taxa into two groups: the first with high
272 activity (with the prefix "hyper" for high), which would include a smaller fraction of the
273 total taxa, and the second with low activity (prefix "hypo" for low), which would include
274 a larger fraction of the total taxa. That assumption is based on the hypothesis that at any
275 one time, most taxa within a natural community are not very active and only a relatively
276 small fraction of the organisms are very active (24). We set the cutoff response to
277 separate high and low activity taxa at a value of 50% of the maximum, which
278 corresponded to a relatively high percent change (Fig. S1b).

279 The second procedure to assign phylotypes to guilds involved the examination of
280 their relative substrate incorporation with the three different concentrations tested. For
281 each taxon, we determined if their isotopic incorporation was significantly different with

different substrate concentrations. This was carried out by an F-test of significantly different slopes from the regression line of fluorescence versus enrichment (i.e. significantly different HCE values). Taxa with no significantly different isotopic incorporation among the three concentrations were named eurytrophs ("eury" = "wide" concentration optimum). Taxa with higher incorporation at the highest concentration(s) were named copiotrophs ("copio" = "many" or high concentration optimum). Taxa with higher incorporation at the lower concentration(s) were named oligotrophs ("oligo" for "few" or low concentration optimum). Taxa with higher isotopic incorporation at the intermediate concentration were named mesotrophs ("meso" for "middle" concentration), and taxa with higher isotopic incorporation at the high and low concentrations (at the extremes) were named allotrophs ("allo" for "different" concentrations). The naming scheme is summarized in Fig. S2. Following guild assignment, all guilds were plotted on ternary diagrams (baricentric plots where for each taxon, the HCEs for the three concentrations add up to the same constant). Trophic guilds were also mapped onto a maximum parsimony phylogenetic tree of the 16S sequences targeted by the array to examine the phylogenetic distribution of these traits. To statistically test the phylogenetic distribution of trophic lifestyles on the tree, individual characters states (copiotrophic vs. not copiotrophic, oligotrophic vs. not oligotrophic, etc.) were randomly reshuffled 1000 times, and for each reshuffling, a parsimony score (number of character state changes was calculated). This was carried out with the software package Mesquite (25). The parsimony score of the real character distribution was compared to this null distribution.

Acknowledgements

We thank L. Nittler for software development. This work was supported by LLNL LDRD funding (grant # 11-ERD-066) and the DOE-BER Genomic Sciences Program (grant # SCW1039). Work was performed under the auspices of the U.S. Department of Energy at Lawrence Livermore National Laboratory under Contract DE-AC52-07NA27344.

Fig. 1: Pairwise comparisons of relative incorporation of isotopically labeled AAs by 107 16S rRNA phylotypes from SF Bay at three concentrations (high, medium, and low). Each data point represents the HCE (hybridization corrected enrichment) for a probe set (delta permil divided by fluorescence). Error bars indicate the standard errors of the slope calculation. Blue labels on panel a) display the relative positions of 5 trophic strategies in relation to the regression (blue) line.

Fig. 2: Ternary plots taking into account the three amino acid concentrations showing the relative responses by all phylotypes (a) which were subsequently grouped into guilds (b-e) according to statistical tests. Background color shows the area of the plot representing theoretical guilds (yellow = mesotroph; red = copiotroph; green = oligotroph; orange = allotroph)

Fig. 3: Trophic strategy identified by statistical analysis of relative AA incorporation mapped onto a maximum parsimony unrooted 16S rRNA gene phylogeny. Ancestral states were identified by parsimony.

Fig. S1: a) Distribution of HCE values (i.e. relative isotopic incorporation, or activity) for 107 microbial taxa incubated with 5 μM ^{15}N-labeled AAs, and b) percent decrease of those values. The arrow indicates the cutoff value used to distinguish highly active and less active taxa, where a local high in percent decrease occurred in the distribution (this corresponds to 50% of the maximum).

Fig. S2: Flowchart of model used to classify microbial groups into guilds based on the relative incorporation of labeled AAs at three concentrations. HCE (hybridization-corrected enrichment) represents the relative isotopic enrichment of each taxon as described in the methods. We used the HCE value of 50% of the maximum as a cutoff to distinguish active (hyper) and less active (hypo) taxa (see Fig. S1).

Fig. S3: Results of phylogenetic distribution of copiotrophy on the 16S phylogeny, showing the frequency distribution of parsimony scores from 1000 randomly shuffled character states. The parsimony score for the actual dataset is labeled with the arrow and was significantly different from the null distribution.

Fig. S4: Relative isotopic enrichment of 107 microbial taxa from ^{15}N-enriched amino acids at three concentrations, color-coded from yellow (high) to white (medium) to blue (low). Taxa names refer to ribosomal phylotypes and were assigned to guilds based on a simple statistical model (see Fig. S2).

References

1. Whitman WB, Coleman DC, & Wiebe WJ (1998) Prokaryotes: the unseen majority. *Proc Natl Acad Sci USA* 95:6578-6583.
2. Azam F (1998) Microbial control of oceanic carbon flux: the plot thickens. *Science* 280(5364):694-696.
3. Nissen H, Nissen P, & Azam F (1984) Multiphasic uptake of D-glucose by an oligotrophic marine bacterium. *Mar Ecol Prog Ser* 16:155-160.
4. Stocker R, Seymour JR, Samadani A, Hunt DE, & Polz MF (2008) Rapid chemotactic response enables marine bacteria to exploit ephemeral microscale nutrient patches. *Proc Natl Acad Sci USA* 105(11):4209-4214.
5. Martens-Habbena W, Berube PM, Urakawa H, de la Torre JR, & Stahl DA (2009) Ammonia oxidation kinetics determine niche separation of nitrifying Archaea and Bacteria. *Nature* 461(7266):976-979.
6. Suttle C, Fuhrman JA, & Capone DG (1990) Rapid ammonium cycling and concentration-dependent partitioning of ammonium and phosphate: implications for carbon transfer in planktonic communities. *Limnol Oceanogr* 35:424-433.
7. Alonso C & Pernthaler J (2006) Concentration-dependent patterns of leucine incorporation by coastal picoplankton. *Appl Environ Microbiol* 72(3):2141-2147.
8. Koch AL (2001) Oligotrophs versus copiotrophs. *BioEssays* 23(7):657-661.
9. Polz MF, Hunt DE, Preheim SP, & Weinreich DM (2006) Patterns and mechanisms of genetic and phenotypic differentiation in marine microbes. *Phil Trans R Soc B* 361(1475):2009-2021.
10. Lauro FM*, et al.* (2009) The genomic basis of trophic strategy in marine bacteria. *Proc Natl Acad Sci USA* 106(37):15527-15533.
11. Fuhrman JA & Azam F (1980) Bacterioplankton secondary production estimates for coastal waters of British Columbia, Canada, Antarctica, and California, USA. *Appl Environ Microbiol* 39(6):1085-1095.
12. Poretsky RS, Sun S, Mou X, & Moran MA (2010) Transporter genes expressed by coastal bacterioplankton in response to dissolved organic carbon. *Envir Microbiol* 12(3):616-627.
13. Mayali X*, et al.* (2012) High-throughput isotopic analysis of RNA microarrays to quantify microbial resource use *ISME J* 6:1210-1221.
14. Evens R & Braven J (1988) A seasonal comparison of the dissolved free amino acid levels in estuarine and English Channel waters. *Sci Total Environ* 76:69-78.
15. Buchan A, Gonzàlez JM, & Moran MA (2005) Overview of the marine *Roseobacter* lineage. *Appl Environ Microbiol* 71(10):5665-5677.
16. Newton RJ*, et al.* (2010) Genome characteristics of a generalist marine bacterial lineage. *ISME J* 4(6):784-798.

17. Lande R & Arnold SJ (1984) The measurement of selection on correlated characters. *Evolution* 37(6):1210-1226.
18. Hunt DE*, et al.* (2008) Resource partitioning and sympatric differentiation among closely related bacterioplankton. *Science* 320(5879):1081-1085.
19. Kujawinski EB (2011) The Impact of Microbial Metabolism on Marine Dissolved Organic Matter. *Annual Review of Marine Science* 3(1):567-599.
20. Eichinger M, Poggiale JC, & Sempéré R (2011) Toward a mechanistic approach to modeling bacterial DOC pathways: a review. *Microbial carbon pump in the ocean*, eds Jiao N & Azam F (Science/AAAS, Washington D.C.).
21. Ratkowsky DA, Olley J, McMeekin TA, & Ball A (1982) Relationship between temperature and growth rate of bacterial cultures. *J Bacteriol* 149(1):1-5.
22. Rouder JN*, et al.* (2008) An assessment of fixed-capacity models of visual working memory. *Proc Natl Acad Sci USA* 105(16):5975-5979.
23. Singh-Gasson S*, et al.* (1999) Maskless fabrication of light-directed oligonucleotide microarrays using a digital micromirror array. *Nat Biotech* 17(10):974-978.
24. Smith EM & del Giorgio PA (2003) Low fractions of active bacteria in natural aquatic communities? *Aquat Microb Ecol* 31(2):203-208.
25. Maddison WP & Madison DR (2011) Mesquite: a modular system for evolutionary analysis), 2.75.

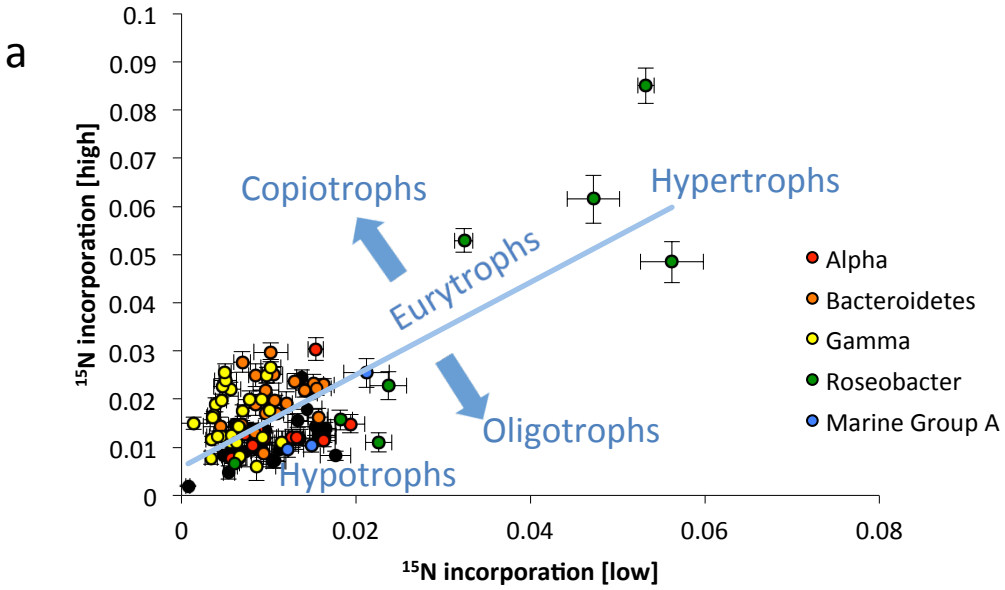
a
0.1
0.09
0.08
0.07
0.06
0.05
0.04
0.03
0.02
0.01
0
15N incorporation [high]
Copiotrophs
Hypertrophs
Eurytrophs
Oligotrophs
Hypotrophs
Alpha
Bacteroidetes
Gamma
Roseobacter
Marine Group A
0
0.02
0.04
0.06
0.08
15N incorporation [low]

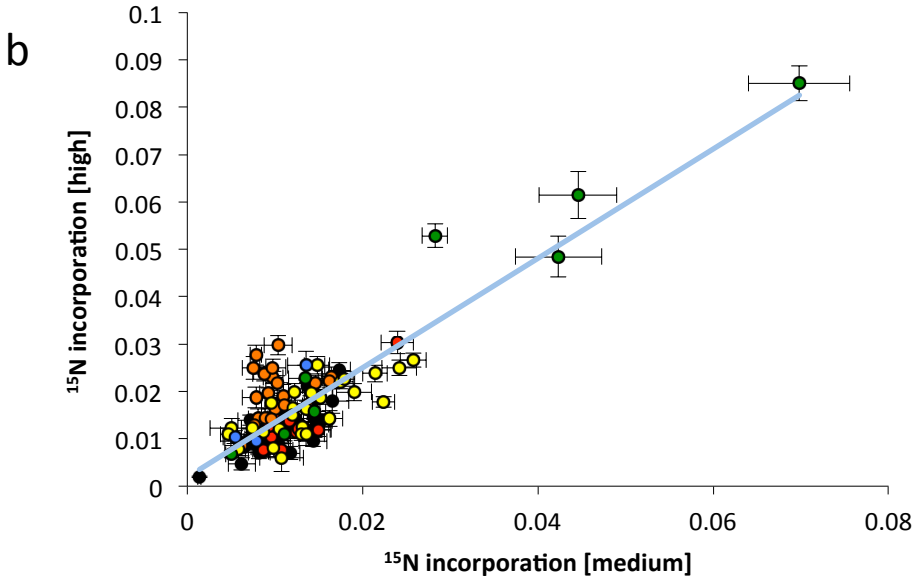
b
0.1
0.09
0.08
0.07
0.06
0.05
0.04
0.03
0.02
0.01
0
15N incorporation [high]
0
0.02
0.04
0.06
0.08
15N incorporation [medium]

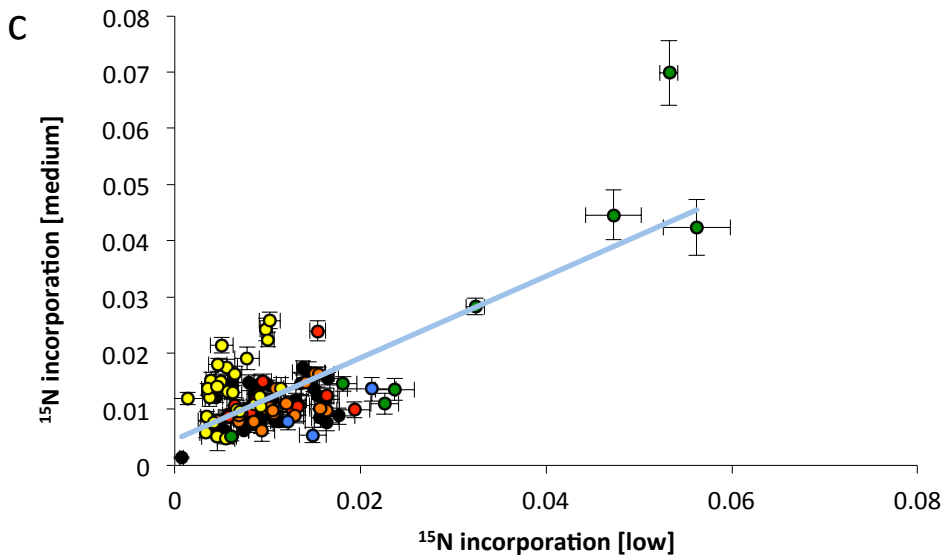
c
0.08
0.07
0.06
0.05
0.04
0.03
0.02
0.01
0
15N incorporation [medium]
0
0.02
0.04
0.06
0.08
15N incorporation [low]

Fig. 1

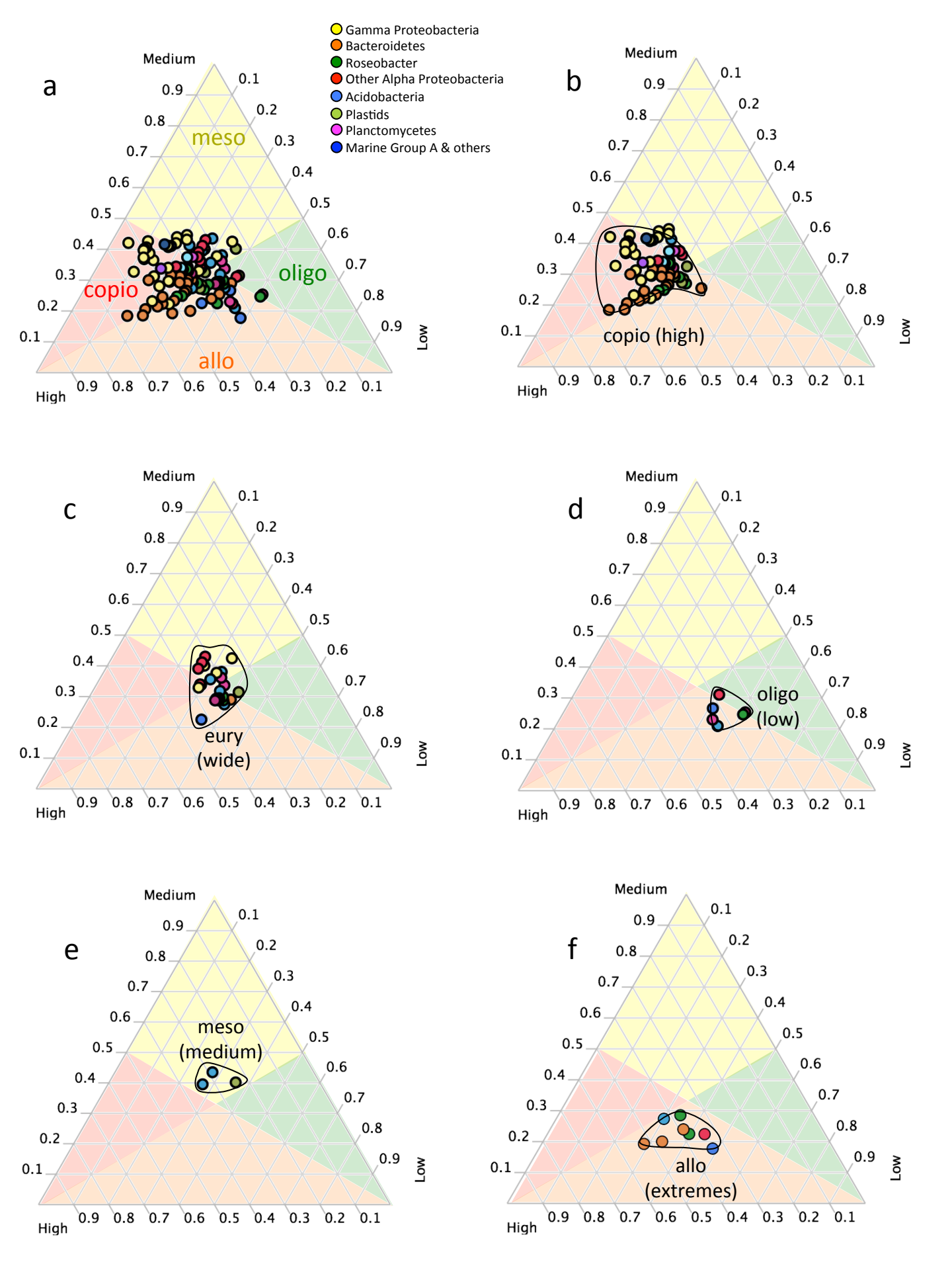
Gamma Proteobacteria
Bacteroidetes
Roseobacter
Other Alpha Proteobacteria
Acidobacteria
Plastids
Planctomycetes
Marine Group A & others
a
Medium
meso
copio
oligo
allo
High
Low
b
copio (high)
c
eury
(wide)
d
oligo
(low)
e
meso
(medium)
f
allo
(extremes)

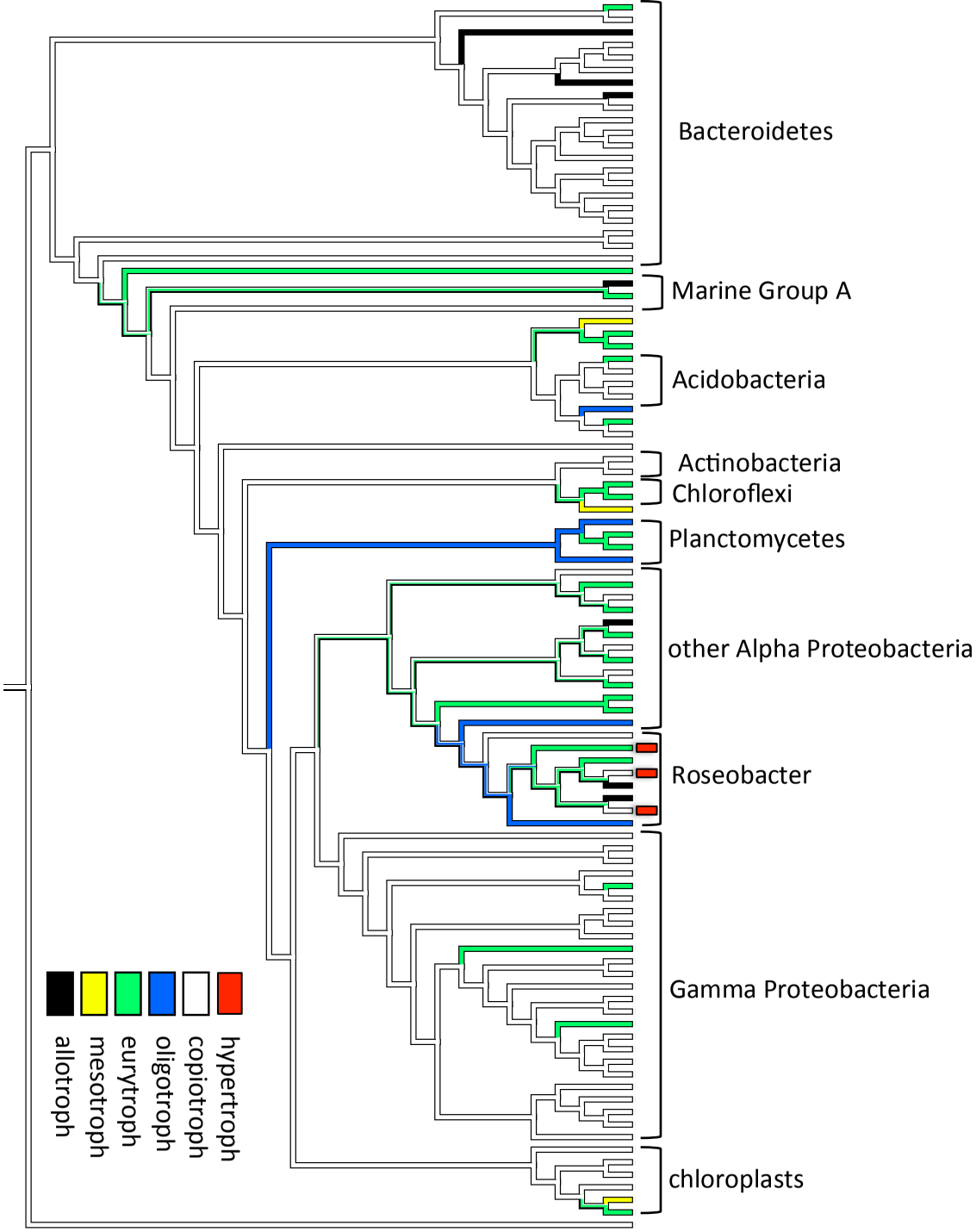
Bacteroidetes
Marine Group A
Acidobacteria
Actinobacteria
Chloroflexi
Planctomycetes
other Alpha Proteobacteria
Roseobacter
Gamma Proteobacteria
chloroplasts
allotroph
mesotroph
eurytroph
oligotroph
copiotroph
hypertroph

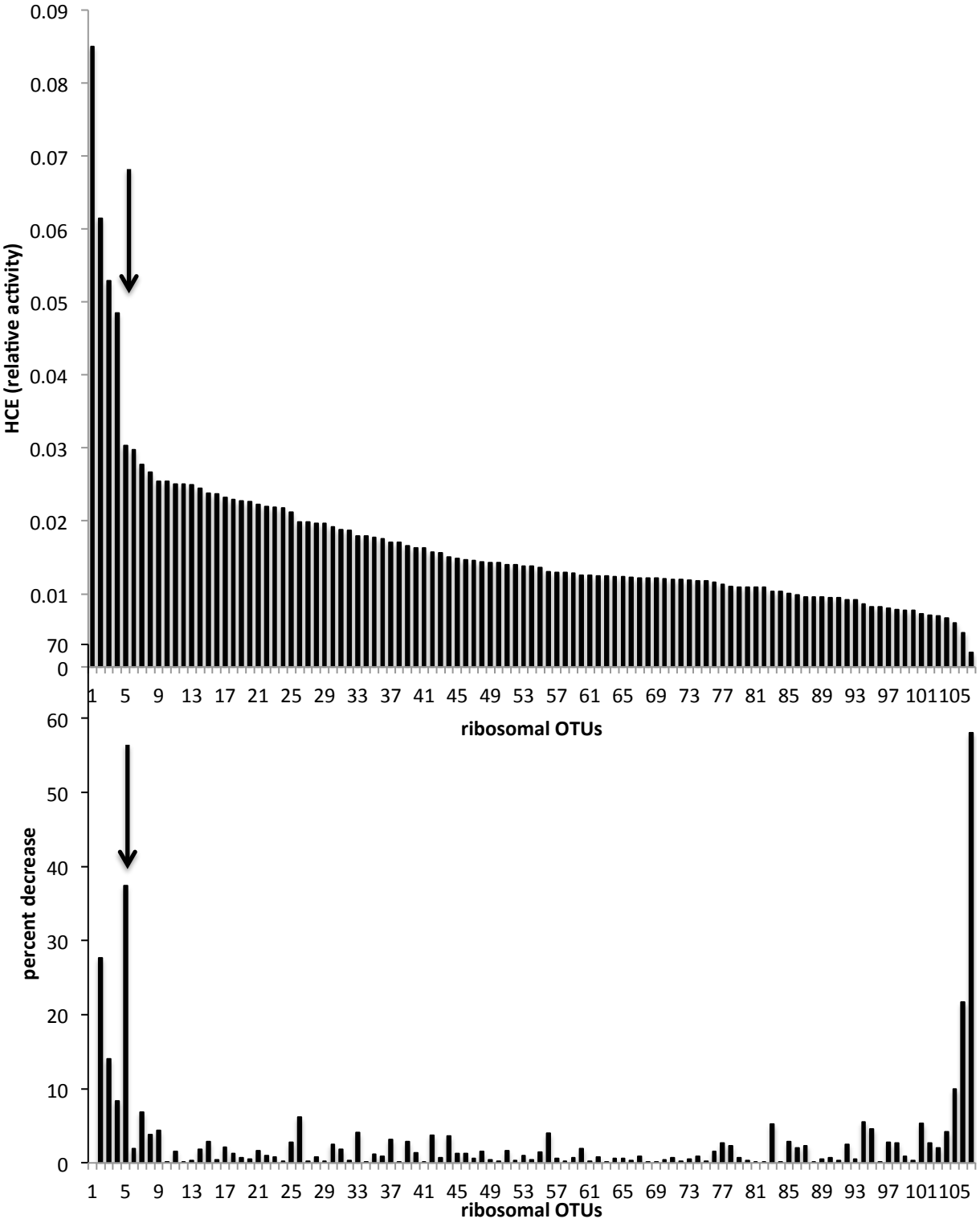
HCE (relative activity)
0.09
0.08
0.07
0.06
0.05
0.04
0.03
0.02
0.01
70
0
1 5 9 13 17 21 25 29 33 37 41 45 49 53 57 61 65 69 73 77 81 85 89 93 97 101105
ribosomal OTUs
percent decrease
60
50
40
30
20
10
0
1 5 9 13 17 21 25 29 33 37 41 45 49 53 57 61 65 69 73 77 81 85 89 93 97 101105
ribosomal OTUs

Fig. S1

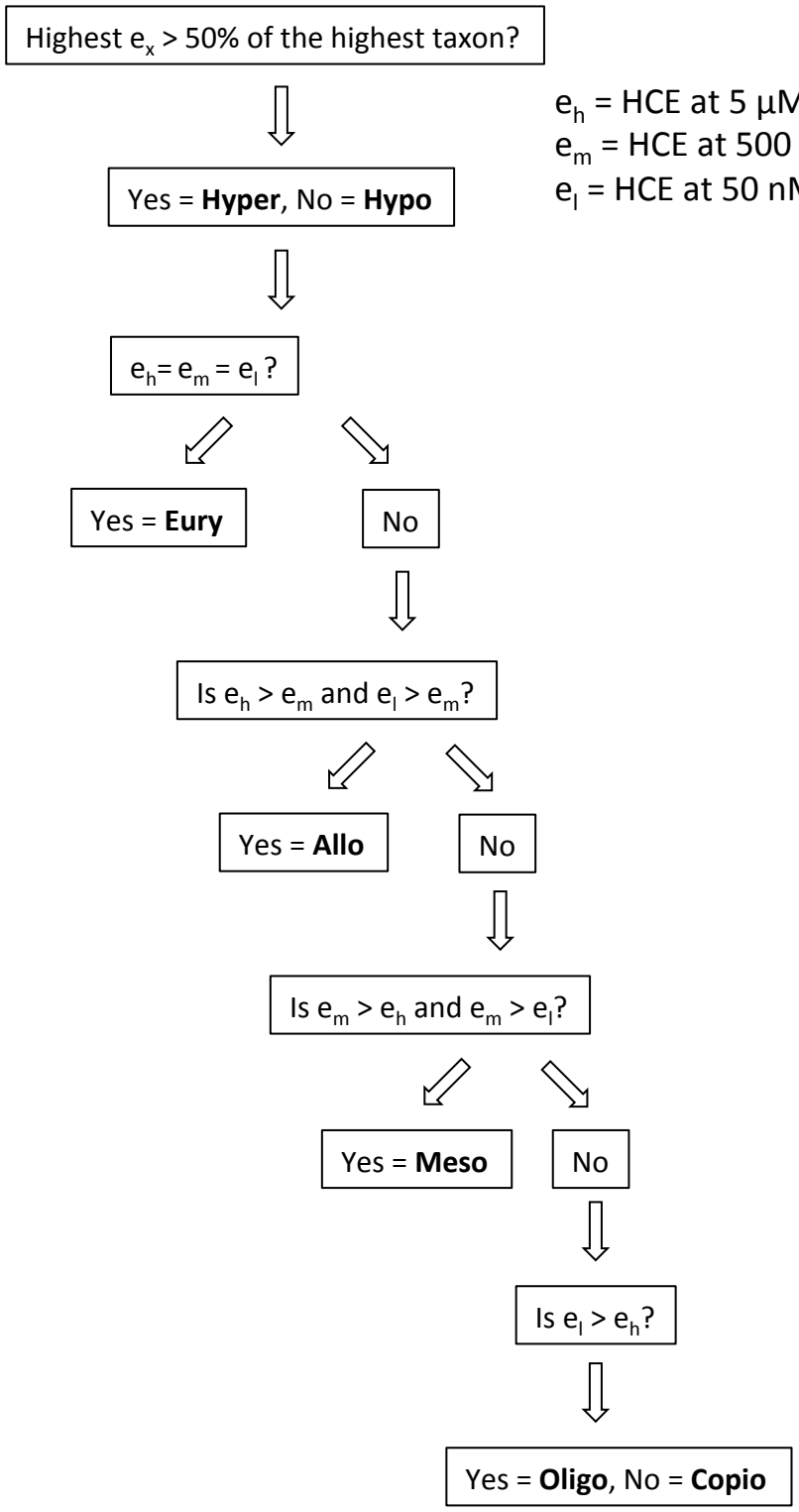
Highest e_x > 50% of the highest taxon?
Yes = **Hyper**, No = **Hypo**
e_h = HCE at 5 µM
e_m = HCE at 500 nM
e_l = HCE at 50 nM
$e_h = e_m = e_l$?
Yes = **Eury**
No
Is $e_h > e_m$ and $e_l > e_m$?
Yes = **Allo**
No
Is $e_m > e_h$ and $e_m > e_l$?
Yes = **Meso**
No
Is $e_l > e_h$?
Yes = **Oligo**, No = **Copio**

Fig. S2

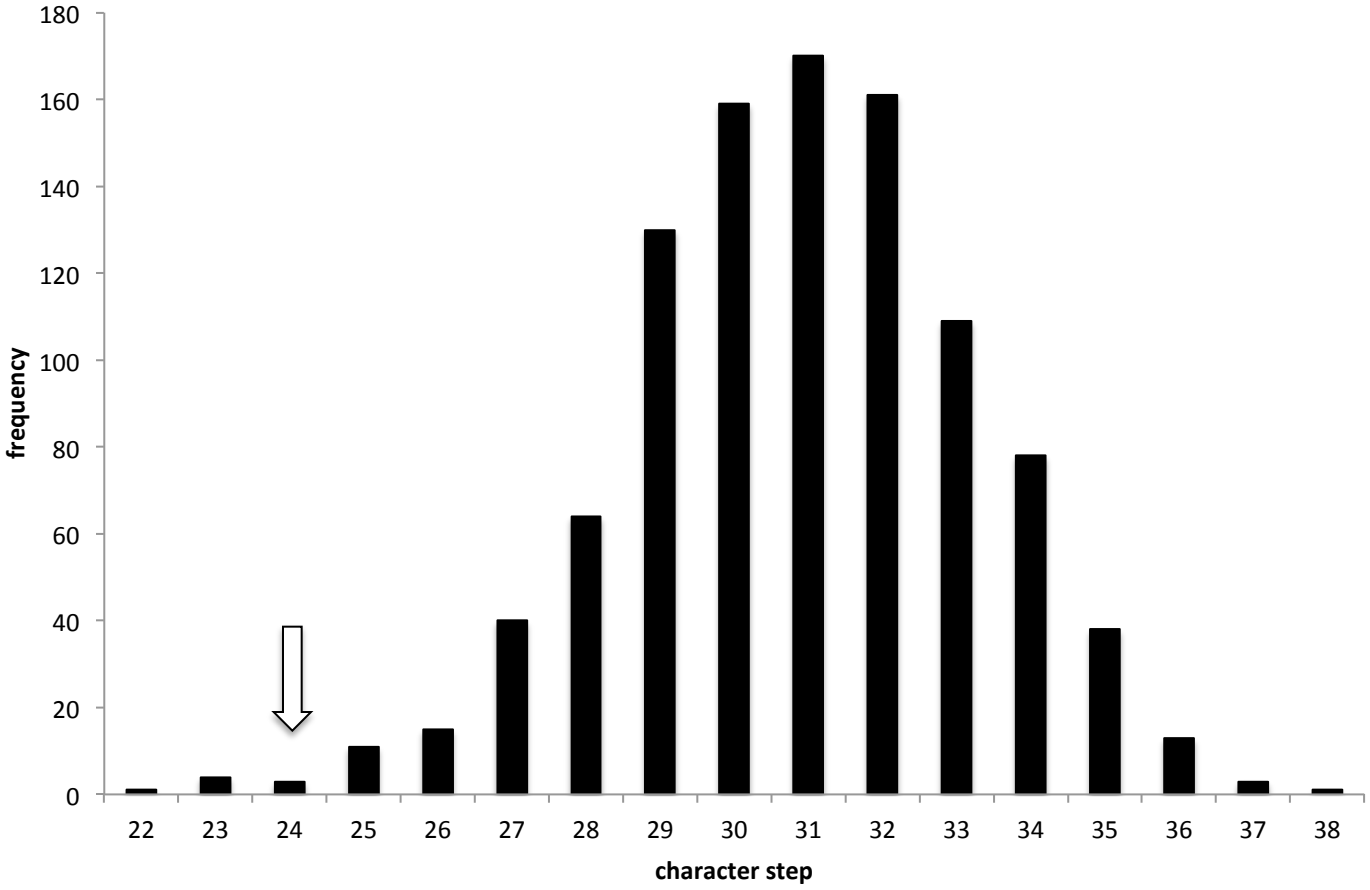
180
160
140
120
100
80
60
40
20
0
frequency
22
23
24
25
26
27
28
29
30
31
32
33
34
35
36
37
38
character step

Fig. S3

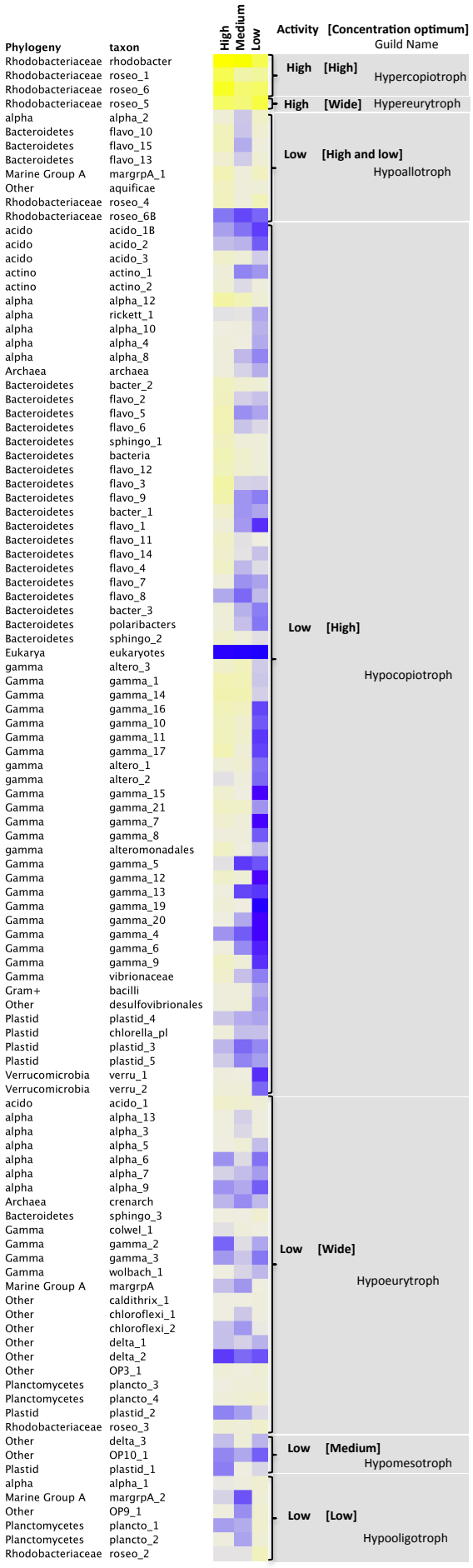
High
Medium
Low
Activity
[Concentration optimum]
Guild Name
Phylogeny
taxon
High [High] Hypercopiotroph
High [Wide] Hypereurytroph
Low [High and low] Hypoallotroph
Low [High] Hypocopiotroph
Low [Wide] Hypoeurytroph
Low [Medium] Hypomesotroph
Low [Low] Hypooligotroph

Fig. S4